Applications of the Theory of Optical Spectroscopy to Numerical Simulations

M. MILOSEVIC* and S. L. BERETS†
Harrick Scientific Corporation, P.O. Box 1288, 88 Broadway, Ossining, New York 10562

A numerical simulation has been developed to extract the optical constants from experimental spectra. In particular, transmission, internal reflection, and external reflection spectra can be simulated for any incident angle, polarization, and sample thickness. The simulation is used here to determine the optical constants of two materials and to illustrate differences in spectral features that arise from variations in experimental conditions. Other potential applications of this method include determining film thicknesses from experimental data, selecting the best spectroscopic technique for a particular sample, and cross-referencing spectroscopic techniques.

Index Headings: **Spectroscopy; Internal reflection; External reflection; Transmission; Numerical simulations; Optical constants.**

INTRODUCTION

Optical spectroscopy is routinely used to identify and characterize compounds, to analyze complex mixtures, and to follow chemical reactions. The usefulness of this technique results from the characteristic and distinctive interaction of each compound with electromagnetic radiation. Experimental results, however, are highly dependent on the specific conditions including the spectroscopic technique, the geometry of the sample, the polarization of the incident radiation, and the angle at which the incident radiation impinges on the sample. Relevant information can be extracted from the experiment in the form of the optical constants. Since the optical constants are independent of the experimental method used, they are ideal for characterizing compounds and cross-referencing results obtained under different experimental conditions. The optical constants are a direct consequence of the interaction of radiation and matter and thus provide insight into the molecular structure of a material.

The relationship between the optical constants and the spectroscopic observables, although exact, is very complex. Thus, extracting the optical constants from measured data is not straightforward. Three approaches have been taken previously: the two-measurement method,[1-9] the Kramers-Kronig analysis,[8-13] and the harmonic oscillator parameterization.[14-19] In the first approach, at least two independent measurements are made by changing one experimental parameter, such as the incident angle, the polarization, etc. These spectra are then used to calculate n and κ. The two-measurement approach typically reproduces one optical constant more accurately than the other[20,21] and is dependent on the experimental method. The second approach, the Kramers-Kronig transform, is used either in conjunction with this first method or separately to analyze normal incidence reflectance data. Since Kramers-Kronig relates n and κ to each other, it is more accurate than the first method. However, when used alone, the Kramers-Kronig approach is restricted to a specific experimental technique. The third alternative parameterizes the functional form of the dependence of the optical constants on wavenumber using a harmonic oscillator model. This method simultaneously determines n and κ from the same small set of parameters, and the optical constants automatically satisfy Kramers-Kronig. The small parameter set provides a concise format for storing the data and also provides insight into the molecular structure. This parameterization approach compares favorably to the other techniques.[14-16] However, previous work has limited it to specific applications.

This paper describes a numerical method for extracting the optical constants from transmission, internal reflection, and external reflection spectra. It first describes enhancements made to the harmonic oscillator parameterization and details the fundamental theory relating the optical constants to the spectroscopic observables, transmittance and reflectance. It then demonstrates extraction of the optical constants from the experimental spectra of polyethylene and glass. Finally, these optical constants are used to simulate spectra under a variety of conditions to illustrate potential applications.

THE THEORY OF OPTICAL SPECTROSCOPY

The relationship between the optical constants and the reflectance and transmittance of the material is described herein. This is accomplished in several stages. First, the molecular vibrations of the sample are modeled and the effect of an applied external electric field is described. This step provides the functional form of the dependence of the optical constants on wavenumber. Next, the propagation of radiation through the sample is developed by examining its propagation through an absorbing medium, an interface, a plane-parallel sample, and a multilayer. This step relates the optical constants to the spectroscopic observables and hence the molecular vibrations to the reflectance and transmittance of the sample.

Modeling the Molecular Vibrations. Each molecule has an internal energy, U, which can be expressed in terms of the coordinates of its atoms. Linear and nonlinear molecules consisting of N atoms require $3N - 5$ and $3N - 6$ degrees of freedom, respectively, to describe their translational, rotational, and vibrational motions. Thus a set of generalized coordinates, G_i, can be found that completely describes the internal motions of the mole-

Received 1 December 1990; revision received 20 November 1992.
* Present address: Spectra-Tech, 652 Glenbrook Road, Stamford, CT 06906.
† Author to whom correspondence should be sent.

0003-7028/93/4705-0566$2.00/0

cule. The internal energy of a molecule can then be written as:

$$U = U(G_1, \ldots, G_b) \tag{1}$$

where b is the total number of degrees of freedom per molecule.

For small oscillations of the atoms around the equilibrium position, U can be expressed as a Taylor series expansion in generalized coordinates:

$$U = U_0 + \frac{1}{2}\sum_{ij} \frac{\partial^2 U}{\partial G_i' \partial G_j'} G_i' G_j' + \ldots \tag{2}$$

for all j and i from 1 to b. The G_i' are defined as:

$$G_i' = G_i - G_{i0} \tag{3}$$

and G_{i0} are the generalized internal coordinates of the atoms in their equilibrium state. The first term of Eq. 2, U_0, is the internal potential energy of the molecule in the equilibrium state. Since the molecule is near equilibrium, the first-derivative term of the Taylor series is zero. The second-derivative term, $\frac{\partial^2 U}{\partial G_i' \partial G_j'}$, can be interpreted as a matrix element of some matrix $\mathbf{\Pi}$. The matrix $\mathbf{\Pi}$ is symmetric since $\frac{\partial^2 U}{\partial G_i' \partial G_j'} = \frac{\partial^2 U}{\partial G_j' \partial G_i'}$. This symmetric matrix can be diagonalized with the use of a unitary transformation V. This procedure introduces a new set of b generalized coordinates, X_ξ:

$$X_\xi = \sum_\beta V_{\xi\beta} G_\xi' \tag{4}$$

such that

$$V^\dagger \mathbf{\Pi}\, V = \Omega \tag{5}$$

where Ω is the diagonal matrix. Equation 2 can be rewritten as:

$$U = U_0 + \frac{1}{2}\sum_\xi X_\xi^2 \Omega_{\xi\xi} + \ldots . \tag{6}$$

While Eq. 2 describes a complex system of strongly coupled harmonic oscillators, Eq. 6 describes a system of weakly coupled (nearly noninteracting) harmonic oscillators. The second term of Eq. 6 represents the contribution to the potential energy from the fundamental collective vibrational modes, while the cubic and higher terms are responsible for combinations, differences, and overtones. For small oscillations, the cubic and higher-order terms of Eq. 6 are negligible, and the system can be described as a collection of independent harmonic oscillators.

This decomposition of coupled harmonic oscillators into a collection of independent oscillators is known as a normal-mode expansion, and the independent oscillators are called normal modes. Each normal mode represents a different collective vibrational state of the molecule and is a linear combination of the original coupled harmonic vibrations.[22]

The Effect of an External Electric Field on the Molecular Vibrations. When one of these independent oscillators is exposed to an electromagnetic field, it becomes polarized. The electric field distorts the charge distribution within the molecule, inducing a dipole moment. The forces which bond the atoms within the molecule resist this disturbance and produce a restoring force. Energy losses from the excited normal mode also occur due to radiation damping and energy transfer to the other modes through the higher-order terms of the potential energy. These losses damp the harmonic oscillations of the normal mode described by Eq. 6.

Thus, a normal mode can be described by the equation of motion for a damped harmonic oscillator in an electric field, **E**:

$$\mathbf{E}q = m\left(\frac{\mathrm{d}^2\mathbf{x}}{\mathrm{d}t^2} + \gamma\frac{\mathrm{d}\mathbf{x}}{\mathrm{d}t} + \omega_0^2\mathbf{x}\right) \tag{7}$$

where $\mathbf{x}$ is the displacement parallel to the field. The $m\omega_0^2\mathbf{x}$ is the harmonic restoring force, m is the reduced mass of the normal mode oscillator, q is the charge on that oscillator, and γ is the damping coefficient.

The displacement of the oscillator varies with the same frequency ω as the applied electric field. Thus the equation of motion (Eq. 7) can be solved for $\mathbf{x}$, giving:

$$\mathbf{x} = \frac{q/m}{\omega_0^2 - \omega^2 + \mathrm{Im}\gamma\omega}\mathbf{E}. \tag{8}$$

Note that the strength of the interaction between the electric field and the oscillator depends on the difference between the frequency of the electric field, ω, and the characteristic frequency of the oscillator, ω_0.

The dipole moment induced by the external electric field, $\mathbf{p}$, is a product of the charge and the displacement, i.e., $\mathbf{p} = q\mathbf{x}$. Substituting this into Eq. 8 gives:

$$\mathbf{p} = \frac{q^2/m}{\omega_0^2 - \omega^2 + \mathrm{Im}\gamma\omega}\mathbf{E}. \tag{9}$$

Since the induced dipole is proportional to $\mathbf{E}$, it can be expressed as $\mathbf{p} = \alpha(\omega)\mathbf{E}$, where $\alpha(\omega)$ is defined as the polarizability. Rearranging Eq. 9 gives a polarizability of:

$$\alpha(\omega) = \frac{q^2/m}{\omega_0^2 - \omega^2 + \mathrm{Im}\gamma\omega}. \tag{10}$$

Since the j normal modes are independent, the molecular polarizability is given by the sum:

$$\alpha(\omega) = \alpha_0 + \frac{e^2}{m_p}\sum_{j=1}^{b} \frac{f_j/\mu_j}{\omega_j^2 - \omega^2 + \mathrm{Im}\gamma_j\omega} \tag{11}$$

where the jth normal-mode oscillator has an oscillator strength (f_j), a frequency (ω_j), a damping coefficient (γ_j), and an effective mass (μ_j). The m_p is the proton mass, and e is the electronic charge. The electronic contribution to the polarizability, α_0, has been separated from the vibrational terms since it can be considered constant in the mid-infrared; i.e., α_0 is independent of ω.

Thus far, only the interaction between the external electromagnetic field and a molecule has been considered. However, the electric field that acts on that molecule results from both the external field and the electric fields of the surrounding molecules. If these surrounding molecules are neglected (i.e., molecules in a rarefied gas), then the polarization of the medium is simply expressed by Eq. 11. As the density of molecules increases, the

molecules come closer together and their interaction has a greater contribution to the internal potential energy. This behavior perturbs the normal modes; e.g., characteristic frequencies shift and damping constants change.

The molecular interaction in a material and the nonlinear behavior of the dielectric constant, ϵ, with concentration are partly described by the well-known Clausius-Mossotti relationship:[23]

$$\epsilon(\omega) = 1 + \frac{4\pi N\alpha(\omega)}{1 - \frac{4\pi N\alpha(\omega)}{3}} \tag{12}$$

where N is the number of molecules per unit volume. The Clausius-Mossotti relationship does not account for all intermolecular interactions but should provide a better estimate than would the neglect of these effects.[19]

The dielectric constant is related to the complex refractive index, n_c, by:

$$n_c(\omega) = \sqrt{\epsilon(\omega)} = n(\omega) + \mathrm{Im}\kappa(\omega) \tag{13}$$

where $n(\omega)$ is the real refractive index of the medium and $\kappa(\omega)$ is the imaginary part of the complex refractive index, also known as the absorption index.

In infrared spectroscopy, frequency is typically measured in wavenumbers, $\bar{\nu}$, which is related to ω by:

$$\omega = 2\pi c\bar{\nu} \tag{14}$$

where c is the speed of light.

Combining Eqs. 11 through 14 gives the optical constants as a function of $\bar{\nu}$ and the polarizability parameters of the normal modes:

$$n_c(\bar{\nu}) = \left(1 + \frac{4\pi N\alpha_0 + \frac{Ne^2}{\pi c^2 m_p}\sum_{j=1}^{b}\frac{f_j/\mu_j}{\bar{\nu}_j^2 - \bar{\nu}^2 + \mathrm{Im}\bar{\nu}\Gamma_j}}{1 - \frac{4\pi N\alpha_0 + \frac{Ne^2}{\pi c^2 m_p}\sum_{j=1}^{b}\frac{f_j/\mu_j}{\bar{\nu}_j^2 - \bar{\nu}^2 + \mathrm{Im}\bar{\nu}\Gamma_j}}{3}} \right)^{1/2} \tag{15}$$

where $\Gamma_j = \gamma_j/2\pi c$. The f_j, μ_j, $\bar{\nu}_j$, and Γ_j are the polarizability parameters of the normal modes of the molecule, and α_0 is the electronic contribution to the polarizability, which can be estimated from the refractive index in the visible spectral region. Note that the mass of a normal mode is on the same order of magnitude as the mass of an atom and is several orders of magnitude larger than the mass of an electron. Thus the electronic contribution to the polarizability is much larger than the vibrational contribution, except near resonant vibrational frequencies.

Equation 15 shows that a set of parameters $\{f_j, \mu_j, \bar{\nu}_j, \Gamma_j, \alpha_0\}$ describes the optical constants, n and κ, of a material at a given wavelength. The optical constants, in turn, are related to the transmittance and reflectance of a material through the Maxwell and Fresnel equations, as discussed below.

Propagation of Radiation through an Absorbing Medium. The propagation of electromagnetic radiation through an absorbing medium is described by Maxwell's equations. Maxwell's equations combine into the wave equation:[23]

$$\left(\frac{\partial^2}{\partial \mathbf{x}^2} - \frac{\epsilon(\omega)}{c^2}\frac{\partial^2}{\partial t^2}\right)\mathbf{E}(\mathbf{x}, t) = 0 \tag{16}$$

where $\mathbf{E}(\mathbf{x}, t)$ is the amplitude of the electric field in position $\mathbf{x}$ at time t, $\epsilon(\omega)$ is the dielectric constant of the medium at frequency ω, and c is the speed of light. Solving Eq. 16 gives:

$$\mathbf{E}(\mathbf{x}, t) = \mathbf{E}_0 e^{\mathrm{Im}\mathbf{k}'\mathbf{x} - \mathrm{Im}\omega t} \tag{17}$$

where $\mathbf{E}_0$ is the amplitude of the electric field at position $\mathbf{x} = 0$ and time $t = 0$. The wave vector $\mathbf{k}'$ points in the direction of propagation of the electromagnetic field, and its magnitude is found by substituting Eq. 17 into Eq. 16. This step gives the dispersion relation:

$$|\mathbf{k}'|^2 = \frac{\epsilon(\omega)\omega^2}{c^2}. \tag{18}$$

Recall from Eq. 13 that the square root of the dielectric constant is the refractive index. Thus if the dielectric constant is a complex quantity, then the refractive index is complex. With the use of Eqs. 13, 14, and 18, the solution to Eq. 17 can be rewritten in terms of the optical constants:

$$\mathbf{E}(\mathbf{x}, t) = \mathbf{E}_0 e^{-2\pi\kappa\bar{\nu}\mathbf{x}} e^{\mathrm{Im}(2\pi n\bar{\nu}\mathbf{x} - \omega t)}. \tag{19}$$

The intensity of the electric field is proportional to the square of the absolute value of the electric field. Thus:

$$I(\mathbf{x}) = I(0)\, e^{-4\pi\kappa\bar{\nu}\mathbf{x}}. \tag{20}$$

Equation 20 is the well-known Lambert law, which describes the absorption of radiation as it propagates through a medium. If $\mathbf{x}$ is chosen in the direction of propagation, then $\bar{\nu}\mathbf{x} = \bar{\nu}x$. Therefore, the intensity of radiation decreases along the propagation direction within the medium. The strength of the absorption is controlled by the imaginary part, κ, of the complex refractive index, n_c. If both parts of the complex refractive index are known, the transmission of an electromagnetic field through a medium can be calculated.

Propagation of Radiation through an Interface. An electromagnetic field at an interface between two media partially reflects and partially transmits (see Fig. 1). Therefore, there are three waves of the form of Eq. 19—incident, transmitted, and reflected:

$$\mathbf{E}_{in}(\mathbf{x}, t) = \mathbf{E}_{in}(0)e^{\mathrm{Im}(2\pi n_1\bar{\nu}_{in}\mathbf{x} - \omega t)} \tag{21a}$$

$$\mathbf{E}_r(\mathbf{x}, t) = \mathbf{E}_r(0)e^{\mathrm{Im}(2\pi n_1\bar{\nu}_r\mathbf{x} - \omega t)} \tag{21b}$$

$$\mathbf{E}_t(\mathbf{x}, t) = \mathbf{E}_t(0)e^{\mathrm{Im}(2\pi n_2\bar{\nu}_t\mathbf{x} - \omega t)} \tag{21c}$$

where n_1 and n_2 are the complex refractive indices which describe the incident and transmitted medium, respectively. From Maxwell's equations, the boundary conditions for these three fields can be deduced. For parallel (p) and perpendicular (s) polarizations of the incident radiation, these conditions are expressed as:

$$E_r^s(0) = r^s E_{in}(0) \tag{22a}$$

$$E_t^s(0) = t^s E_{in}(0) \tag{22b}$$

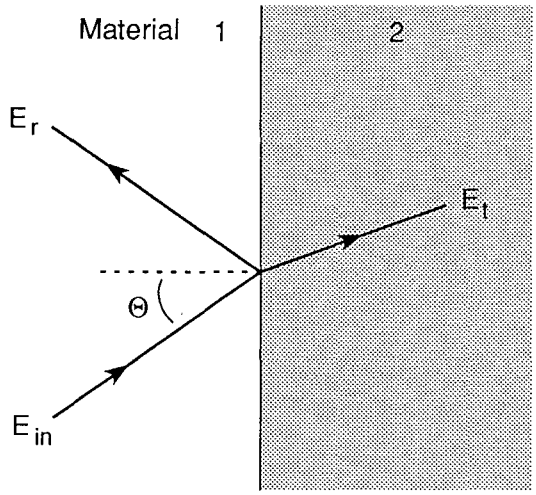

FIG. 1. The reflection and transmission of radiation from a single interface. Arrows indicate the direction of propagation of the radiation.

$$E_r^p(0) = r^p E_{in}(0) \tag{22c}$$

$$E_t^p(0) = t^p E_{in}(0) \tag{22d}$$

where r^s, t^s, r^p, and t^p are the Fresnel amplitude coefficients:

$$r_{12}^p = -\frac{n_2^2\cos\Theta - n_1\sqrt{n_2^2 - n_1^2\sin^2\Theta}}{n_2^2\cos\Theta + n_1\sqrt{n_2^2 - n_1^2\sin^2\Theta}} \tag{23a}$$

$$r_{12}^s = \frac{n_1\cos\Theta - \sqrt{n_2^2 - n_1^2\sin^2\Theta}}{n_1\cos\Theta + \sqrt{n_2^2 - n_1^2\sin^2\Theta}} \tag{23b}$$

$$t_{12}^p = \frac{2n_1n_2\cos\Theta}{n_2^2\cos\Theta + n_1\sqrt{n_2^2 - n_1^2\sin^2\Theta}} \tag{23c}$$

$$t_{12}^s = \frac{2n_1\cos\Theta}{n_1\cos\Theta + \sqrt{n_2^2 - n_1^2\sin^2\Theta}} \tag{23d}$$

and Θ is the angle of incidence.

To relate the Fresnel amplitude coefficients to the transmittance and reflectance of the interface, consider the radiation that impinges on the interface. The power of this radiation must be conserved, that is:

$$P_{in} = P_r + P_t \tag{24}$$

where P_{in}, P_r, and P_t are the power of the incident, reflected, and transmitted radiation respectively. Equation 24 can be rewritten in terms of the energy density, u:

$$u_{in}c_{in}A_{in} = u_rc_rA_r + u_tc_tA_t \tag{25}$$

where c is the speed of light for the specified radiation, and A is the cross-sectional area of that radiation. Relating the speeds of the transmitted and reflected radiation gives:

$$\frac{1}{n_1}u_{in}A_{in} = \frac{1}{n_1}u_rA_r + \frac{1}{n_2}u_tA_t. \tag{26}$$

The areas are related through the incident angle Θ and the refracted angle ϕ such that:

$$u_{in} = u_r + \frac{n_1}{n_2}\frac{\cos\phi}{\cos\Theta}u_t. \tag{27}$$

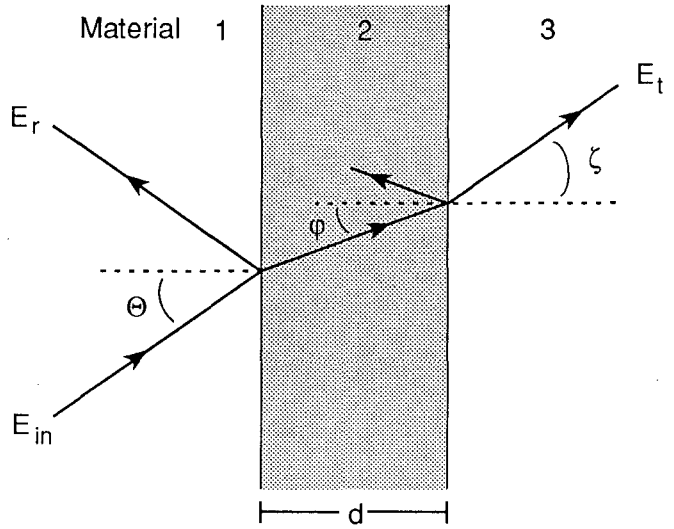

FIG. 2. The reflection and transmission of radiation from a plane-parallel sample. Arrows indicate the direction of propagation of the radiation.

Since $u = \frac{1}{4\pi}E^2$, Eq. 27 can be rewritten as:

$$E_{in}^2 = E_R^2 + \frac{n_1}{n_2}\frac{\sqrt{1 - \sin^2\phi}}{\cos\Theta}E_T^2. \tag{28}$$

With the use of the relationship between the angles Θ and ϕ, in addition to Eqs. 22, Eq. 28 can be expressed as:

$$1 = |r_{12}^i|^2 + \frac{n_1}{n_2}\frac{\sqrt{n_2^2 - n_1^2\sin^2\Theta}}{n_2\cos\Theta}|t_{12}^i|^2 \tag{29}$$

where i stands for the polarization of the incident radiation. Equation 29 reflects the law of conservation of energy; i.e., all radiation is either reflected or transmitted. None of the radiation is absorbed at the interface.

The reflectance, R^i, and transmittance, T^i, of the interface are thus related to the Fresnel amplitude coefficients:

$$R^i = |r_{12}^i|^2 \tag{30a}$$

$$T^i = \frac{n_1}{n_2}\frac{\sqrt{n_2^2 - n_1^2\sin^2\Theta}}{n_2\cos\Theta}|t_{12}^i|^2 \tag{30b}$$

Equations 30 completely express the relationship between the reflecting properties of an interface and the optical constants of the materials on both sides of that interface.

Reflectance and Transmittance of a Plane-Parallel Sample. Assume that a plane-parallel sample of thickness d is sandwiched between two semi-infinite media, as illustrated in Fig. 2. Electromagnetic radiation of the ith polarization (s or p) is incident on the sample through the first medium at an incident angle, Θ.

The form of the solutions (Eqs. 21) for an electromagnetic field inside various media and the boundary conditions (Eqs. 22) completely describe the process illustrated in Fig. 2. Within the sample, there are two components of the electric field. One travels along the incident direction, $\mathbf{E}_+(\mathbf{x}, t)$, and one travels in the op-

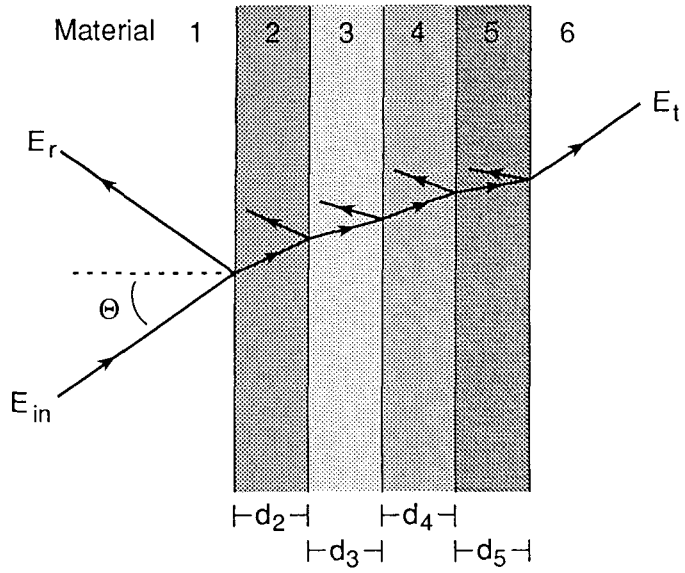

FIG. 3. The reflection and transmission of radiation from a multilayer sample ($k = 6$).

posite direction, $\mathbf{E}_-(\mathbf{x}, t)$. The boundary conditions require that, at the first interface:

$$E_t^i(0) = t_{12}^i E_{in}^i(0) + r_{21}^i E_-^i(0) \tag{31a}$$

$$E_r^i(0) = r_{12}^i E_{in}^i(0) + t_{21}^i E_-^i(0) \tag{31b}$$

and at the second interface:

$$E_-^i(d) = r_{23}^i E_+^i(d) \tag{32a}$$

$$E_t^i(d) = t_{23}^i E_+^i(d) \tag{32b}$$

where r_{23}^i and t_{23}^i are the Fresnel amplitude coefficients at the second interface. These coefficients can be expressed in terms of the angle of incidence on the first interface (Θ) as follows:

$$r_{23}^p = \frac{n_3^2\sqrt{n_2^2 - n_1^2\sin^2\Theta} - n_2^2\sqrt{n_3^2 - n_1^2\sin^2\Theta}}{n_3^2\sqrt{n_2^2 - n_1^2\sin^2\Theta} + n_2^2\sqrt{n_3^2 - n_1^2\sin^2\Theta}} \tag{33a}$$

$$r_{23}^s = \frac{\sqrt{n_2^2 - n_1^2\sin^2\Theta} - \sqrt{n_3^2 - n_1^2\sin^2\Theta}}{\sqrt{n_2^2 - n_1^2\sin^2\Theta} + \sqrt{n_3^2 - n_1^2\sin^2\Theta}} \tag{33b}$$

$$t_{23}^p = \frac{2n_3n_2\sqrt{n_2^2 - n_1^2\sin^2\Theta}}{n_3^2\sqrt{n_2^2 - n_1^2\sin^2\Theta} + n_2^2\sqrt{n_3^2 - n_1^2\sin^2\Theta}} \tag{33c}$$

$$t_{23}^s = \frac{2\sqrt{n_2^2 - n_1^2\sin^2\Theta}}{\sqrt{n_2^2 - n_1^2\sin^2\Theta} + \sqrt{n_3^2 - n_1^2\sin^2\Theta}}. \tag{33d}$$

The solutions to Maxwell's equations relate $E_\pm^i(d)$ and $E_\pm^i(0)$:

$$E_+^i(d) = E_+^i(0)e^{2\mathrm{Im}\pi\bar{\nu}d\sqrt{n_2^2 - n_1^2\sin^2\Theta}} \tag{34a}$$

$$E_-^i(d) = E_-^i(0)e^{-2\mathrm{Im}\pi\bar{\nu}d\sqrt{n_2^2 - n_1^2\sin^2\Theta}} \tag{34b}$$

Using Eqs. 32 through 34, we find that:

$$\rho^i = \frac{E_r^i(0)}{E_{in}^i(0)} = \frac{r_{12}^i + r_{23}^i e^{4\mathrm{Im}\pi\bar{\nu}d\sqrt{n_2^2 - n_1^2\sin^2\Theta}}}{1 + r_{12}^i r_{23}^i e^{4\mathrm{Im}\pi\bar{\nu}d\sqrt{n_2^2 - n_1^2\sin^2\Theta}}} \tag{35a}$$

$$\tau^i = \frac{E_t^i(d)}{E_{in}^i(0)} = \frac{t_{23}^i}{t_{21}^i}(1 - r_{12}^i\rho^i)e^{2\mathrm{Im}\pi\bar{\nu}d\sqrt{n_2^2 - n_1^2\sin^2\Theta}} \tag{35b}$$

where $\bar{\nu}$ is measured in wavenumbers or reciprocal wavelengths.

The spectroscopic observables are:

$$T^i = |\tau^i|^2\frac{n_1}{n_3}\frac{\sqrt{n_3^2 - n_1^2\sin^2\Theta}}{n_3\cos\Theta} \tag{36a}$$

$$R^i = |\rho^i|^2 \tag{36b}$$

where the transmittance, T^i, and reflectance, R^i, are determined by directly substituting Eqs. 35 into Eqs. 36.

The specific choices of the incident angle, the polarization, the optical constants of the three materials, and the spectroscopic technique (internal reflectance, external reflectance, or transmittance) permit descriptions of a broad range of experimental conditions.

Reflectance and Transmittance of Multilayers. This model can be further extended to describe the reflectance and transmittance of a multilayer (see Fig. 3). For a sample with $(k - 1)$ plane-parallel layers each with thickness d_j, the reflectance and transmittance can be written as:

$$R^i = |\rho^i|^2 = \left(\frac{M_{21}}{M_{11}}\right)^2 \tag{37a}$$

$$T^i = |\tau^i|^2 = \left(\frac{1}{M_{11}}\right)^2 \tag{37b}$$

where M_{21} and M_{11} are elements of the matrix $\mathbf{M}$:

$$\mathbf{M} = \begin{pmatrix} 1 & r_{12} \\ r_{12} & 1 \end{pmatrix} \cdot\left(\prod_{j=2}^{k-1}\frac{1}{t_{j;j+1}}\begin{pmatrix} e^{-X_j} & r_{j;j+1}e^{-X_j} \\ r_{j;j+1}e^{X_j} & e^{X_j} \end{pmatrix}\right) \cdot\begin{pmatrix} e^{-X_k} & r_{k;k+1}e^{-X_k} \\ r_{k;k+1}e^{X_k} & e^{X_k} \end{pmatrix} \tag{38}$$

$$X_h = 4\mathrm{Im}\pi\bar{\nu}d_h\sqrt{n_h^2 - n_1^2\sin^2\Theta}. \tag{39}$$

This formulation of Eqs. 36 is extremely useful for modeling materials coated with one or more layers.

For an infinite number ($k \to \infty$) of infinitesimally thin layers ($d_j \to 0$). Eqs. 37 reduce to:

$$R^i = \left|\frac{\sqrt{\xi_i^2 + \beta_i^2}(r_{sub}^i + r_{ire}^i) + [\beta_i(r_{sub}^i - r_{ire}^i) + \xi_i(1 + r_{sub}^i r_{ire}^i)]\cdot\tanh(\sqrt{\xi_i^2 + \beta_i^2})}{\sqrt{\xi_i^2 + \beta_i^2}(1 + r_{sub}^i r_{ire}^i) + [\beta_i(1 - r_{sub}^i r_{ire}^i) + \xi_i(r_{sub}^i + r_{ire}^i)]}\right|^2 \tag{40a}$$

$$T^i = \left|\frac{-\int_0^d \frac{\partial n_{sample}(x)}{\partial x}\frac{n_{sample}(x)}{2(n_{sample}^2(x) - n_{ire}^2\sin^2\theta)}}{\cosh(\sqrt{\xi_i^2 + \beta_i^2})(1 + r_{sub}^i r_{ire}^i) + \sinh(\sqrt{\xi_i^2 + \beta_i^2})\cdot[\beta_i(1 - r_{sub}^i r_{ire}^i) + \xi_i(r_{sub}^i + r_{ire}^i)]}\right|^2 \tag{40b}$$

where r_{sub}^i is the Fresnel amplitude coefficient for the interface between the multilayer and substrate, r_{ire}^i is the

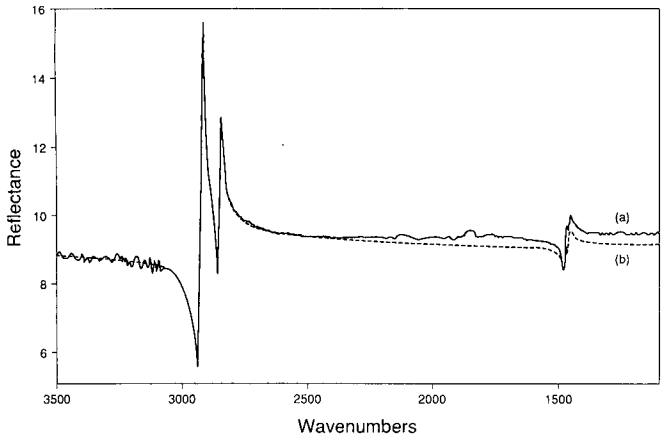

FIG. 4. External reflection spectra of polyethylene (*a*) measured and (*b*) calculated for an incident angle of 45° with *s*-polarization.

Fresnel amplitude coefficient for the interface between material 1 and the multilayer, and $n_{sample}(x)$ is the refractive index of the multilayer at a depth, x, into the material. The ξ_i and β_i from Eqs. 40 are defined as:

$$\xi_s = \int_0^d dx \frac{\partial n_{sample}(x)}{n_{sample}(x)\,\partial x} \cdot \left(1 - \frac{n^2_{sample}(x)}{2(n^2_{sample}(x) - n^2_{ire}\sin^2\theta)}\right) \quad (41a)$$

$$\xi_p = \int_0^d dx \frac{\partial n_{sample}(x)}{\partial x} \frac{n_{sample}(x)}{2(n^2_{sample}(x) - n^2_{ire}\sin^2\theta)} \quad (41b)$$

$$\beta_s = \beta_p = \mathrm{Im} \int_0^d dx \sqrt{n^2_{sample}(x) - n^2_{ire}\sin^2\theta}. \quad (41c)$$

Equations 40 essentially describe the spectroscopic observables across a material where the optical constants vary with the depth into the material. Thus from Eq. 16, which is only valid for homogeneous media, we can describe the reflectance and transmittance of an inhomogeneous material.

EXPERIMENTAL

To illustrate some applications of this model, we examined two samples, polyethylene and glass. A piece of high-density polyethylene was polished for the external reflectance measurements, and a thin slice of the same material was used for the internal reflectance studies. The glass sample was a microscope slide which was used as is.

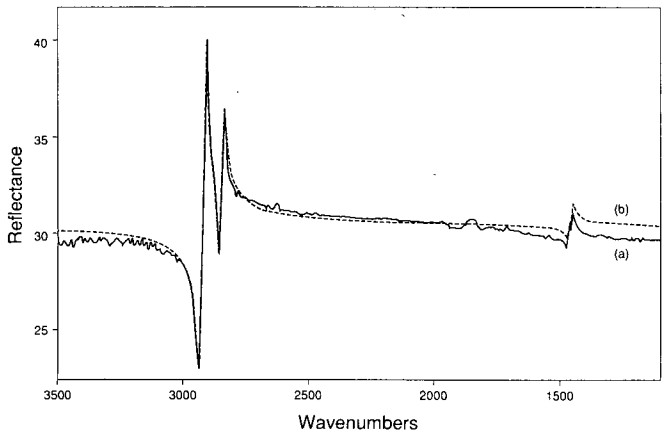

FIG. 5. External reflection spectra of polyethylene at an incident angle of 70° with s-polarized radiation (*a*) measured and (*b*) calculated.

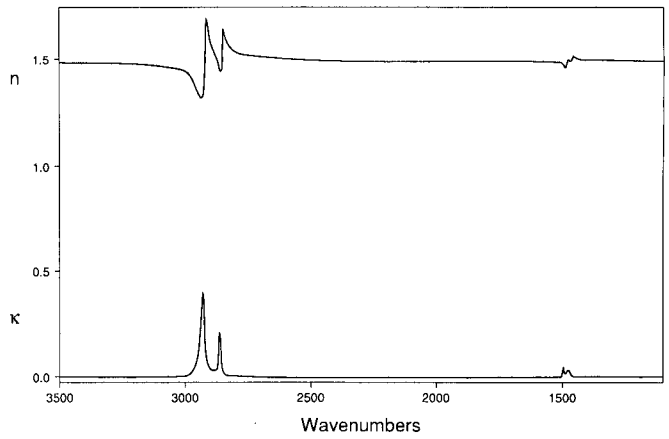

FIG. 6. The optical constants of polyethylene.

External and internal reflection spectra were recorded with a Mattson Polaris spectrometer. For the polyethylene studies, the infrared spectrometer was equipped with the Seagull™‡[24] and two wire-grid polarizers on KRS-5 substrates. Two polarizers were used to ensure a well-defined polarization of the incident beam. The internal reflectance measurements utilized a ZnSe hemispherical internal reflection element (IRE). The reflectance spectrum of glass was measured with the use of Harrick's External Specular Reflection Accessory, which provides a 45° angle of incidence on the sample.

For the experimental measurements, a single-beam reference spectrum, I_0, was recorded under the same conditions as the single-beam sample spectrum, I_s, and the reflectance spectrum ($100*I_s/I_0$) was calculated. For external reflectance, a front-surface aluminum mirror was used as the reference. For internal reflectance, the internal reflection element was the reference material.

The numerical simulations were performed on an "AT" compatible computer using Harrick's SOS™ software package. This package is an implementation of the theoretical approach described herein. Measured spectra were transferred to the simulation with the use of the JCAMP-DX format.[25] Simulated spectra were stored in the JCAMP-DX format and then transferred to Mattson's First™ software for final processing and plotting.

‡ Harrick's variable-angle reflectance accessory.

TABLE I. The polarizability parameters used for polyethylene.[a]

$\bar{\nu}$ (cm^{-1})	Γ_j (cm^{-1})	$\frac{f_j}{\mu_j}$ (amu^{-1})
1458.0	15.0	0.0050
1474.0	5.0	0.0025
2850.0	10.0	0.0450
2885.0	30.0	0.0070
2900.0	30.0	0.0070
2919.8	11.5	0.0980
2930.5	19.0	0.0480

[a] Electronic contribution to the refractive index: 1.49.

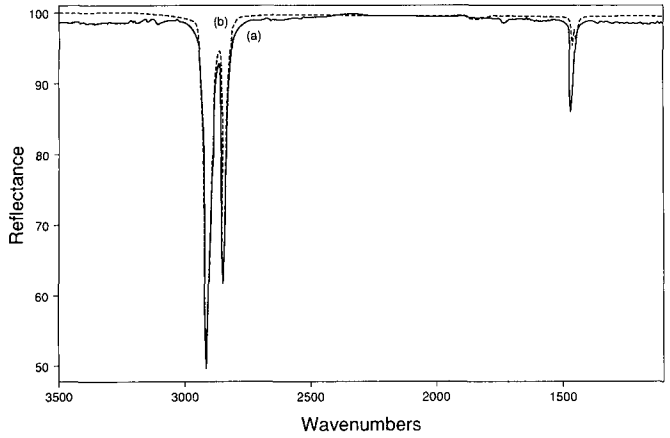

FIG. 7. Internal reflection spectra of polyethylene (*a*) measured and (*b*) calculated for an incident angle of 55° with *s*-polarized radiation.

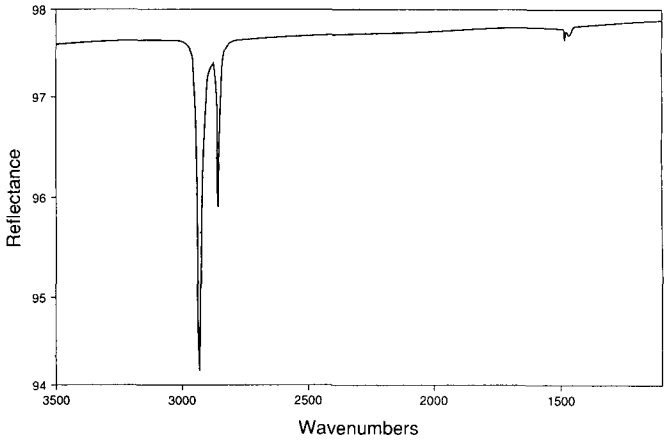

FIG. 9. External reflection spectrum of a 0.1-μm-thick coating of polyethylene on aluminum at an incident angle or 20° with *p*-polarized radiation.

RESULTS AND DISCUSSION

With the use of the model described here, the optical constants for a given sample can be extracted from experimental data. The optical constants can then be used to predict spectral features that result from various experimental conditions, i.e., spectroscopic technique, sample thickness, incident angle, and polarization. In particular, we have applied this model to polyethylene and glass.

Polyethylene. The external reflection spectrum of polyethylene was recorded at 45° with *s*-polarized radiation (see Fig. 4). The calculated spectrum was then fit to the experimental spectrum as follows: For external reflectance, Material 1 is the air (refractive index $n_1 = 1$) that surrounds the polyethylene, Material 2. For an optically thick sample (i.e., $kd \gg 1$), the reflectance from the sample can be described as the reflectance from a single interface (Eq. 30a). An initial guess for the electronic polarizability parameter, α_0, was formulated from the real refractive index of polyethylene at the sodium *D* line,[26] and the reflectance was calculated. The refractive index was then adjusted to account for the average reflectance observed outside the absorption regions. The parameters $\bar{\nu}_j$ and Γ_j were estimated from the experiposition ($\bar{\nu}_j$), and width (Γ_j) were then refined to fit the measured peaks. The best-fit parameters are presented in Table I, and the resulting spectrum is shown in Fig. 4.

The calculated spectrum is a good fit to the experimental data around 3000 cm^{-1} but deviates from it at lower wavenumbers. This observation results from differences between the theoretical model and the experimental conditions. The simulation used calculates the reflectivity at one incident angle, while the observed reflectivity depends on a distribution of angles based on the beam spread of the spectrometer. The model also assumes a perfectly smooth material, but the polyethylene sample was not highly polished. In addition, the reference material was not taken into account. The reference material is generally not perfectly reflective, and its reflectivity is a function of wavenumber.

To confirm that the parameters from Table I provide a good description of the normal modes of polyethylene, we examined a second set of experimental conditions. Figure 5 shows the measured and calculated external reflectance at an incident angle of 70° with *s*-polarization. The differences between these spectra are similar to those of Fig. 4. Hence the selected parameters reproduce the external reflectance of polyethylene and provide a reasonable representation of the polarizability. The optical constants were then calculated from these parameters and are shown in Fig. 6.

Figure 7 compares the calculated and experimental internal reflectance for a 55° incident angle and *s*-polarized radiation. Note that internal reflectance is governed by the same formulae as external reflectance. For internal reflection, Material 1 becomes the IRE on which the sample, Material 2, is pressed. As in the case of the external reflectance measurements, the polyethylene was optically thick, and hence the spectrum can be described by Eq. 30a. The refractive index of the ZnSe IRE was assumed to be 2.42.[26] The fit, shown in Fig. 7, is surprisingly good considering the additional experimental variables introduced by internal reflectance. Since polyethylene is a solid, pressure was applied to achieve good contact between the sample and the IRE. This changed the density of the sample and possibly its structure. In

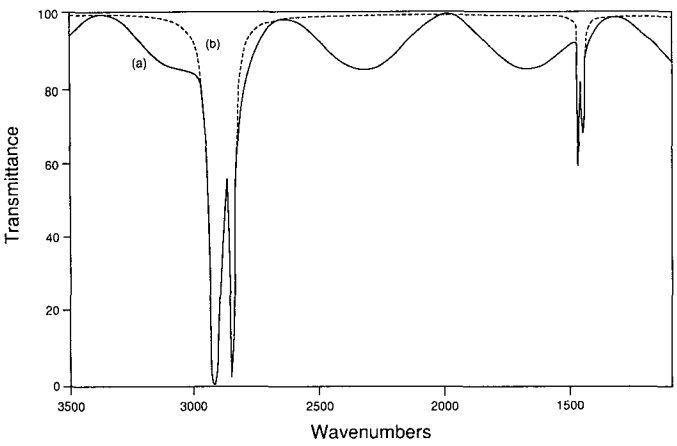

FIG. 8. Transmission spectrum of a 5-μm-thick film of polyethylene calculated at (*a*) normal incidence (Θ = 0°) and (*b*) Brewster's angle (Θ = 55°) with *p*-polarization radiation.

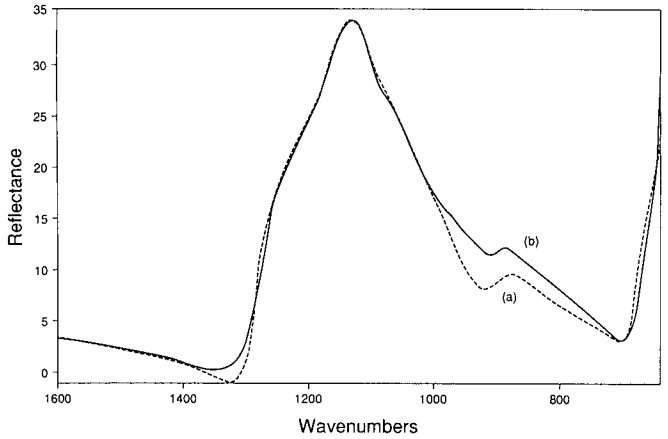

FIG. 10. External reflection spectra of glass (*a*) measured and (*b*) calculated for an incident angle of 45° with unpolarized incident radiation.

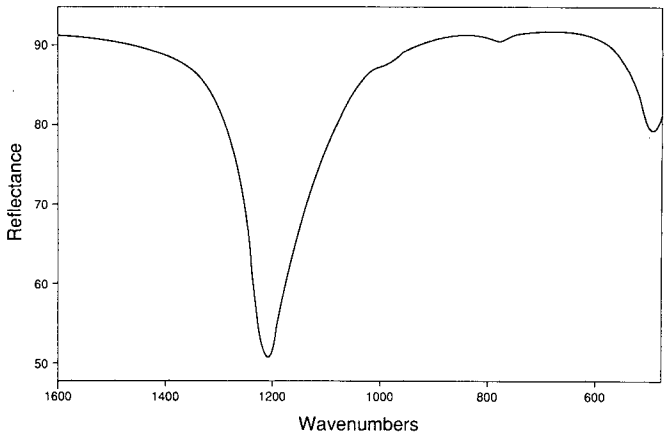

FIG. 11. External reflectance of a 500 Å-thick glass coating on aluminum calculated for a 75° incident angle and *p*-polarized radiation.

addition, the polyethylene may have been oriented, and sample orientation was not maintained during these measurements. These properties affect the polarizability and hence the spectroscopic observables. Thus the sample examined by external reflectance may have differed from that studied by internal reflectance. An additional error was introduced by assuming a constant IRE refractive index. The refractive index is actually a weak function of wavenumber. However, the resulting error from this approximation is expected to be small relative to those mentioned previously.

Figures 8 and 9 illustrate other potential applications of this model, specifically with regard to thin films. For an optically thin material, Material 3, the substance behind the sample (either air or a substrate) must also be considered. Figure 8 shows the transmittance of a free-standing 5 μm-thick polyethylene film at normal incidence ($\Theta = 0°$) and at Brewster's angle ($\Theta = 55°$), calculated from Eq. 36a. Since the film is free-standing, Materials 1 and 3 are air ($n = 1$, $\kappa = 0$). Note that the interference fringes that appear in the normal incidence spectrum do not appear in the spectrum obtained at Brewster's angle.[27,28]

Figure 9 shows the external reflection spectrum of a 0.1-μm-thick film of polyethylene on aluminum, calculated from Eq. 36b for an incident angle of 20° and for *p*-polarization. The refractive index of aluminum (Material 3) as a function of wavenumber was calculated from its plasma frequency.[29] Note that no interference fringes are seen here, as expected.[28]

Glass. In addition to polyethylene, the spectral features of glass were examined. Glass exhibits two bands in the 1300–800 cm^{-1} region, and the more intense band varies depending on the spectroscopic technique.[30] Thus glass was chosen as a test to see whether this behavior could be reproduced.

The external reflectance of an optically thick glass slide was recorded at an incident angle of 45° with unpolarized radiation (Fig. 10). The simulated spectrum was then fit to the experimental data, as described previously. The resulting spectrum is shown in Fig. 10, and the parameters for the fit are listed in Table II. Note that this is not the best fit possible, but it is good enough to illustrate the changes in the glass spectrum with technique.

Using the polarizability parameters from Table II, we calculated the external reflection spectrum of a 500-Å-thick glass film on aluminum for grazing angle and *p*-polarized incident radiation (Fig. 11). The broad band that appeared in the external reflection spectrum of an optically thick sample is now dominated by the band at 1200 cm^{-1}. This band becomes weak relative to the band at 1100 cm^{-1} in transmittance (see Fig. 12). However, both bands can be resolved in the internal reflectance of a thin glass coating on an organic substrate, as demonstrated in Fig. 13. This striking theoretical variation in spectral features due to differences in conditions has been observed experimentally.[30,31]

TABLE II. The polarizability parameters used for glass.[a]

$\bar{\nu}$ (cm^{-1})	Γ_j (cm^{-1})	$\frac{f_j}{\mu_j}$ (amu$_{-1}$)
482	65	0.50
785	50	0.03
990	90	0.09
1090	100	1.11
1140	90	0.63
1180	73	0.30

[a] Electronic contribution to the refractive index: 1.65.

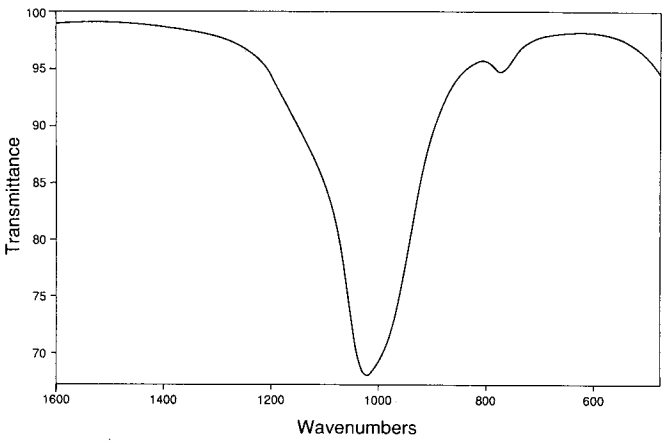

FIG. 12. Simulated normal incidence transmittance of a 0.1-μm-thick glass window.

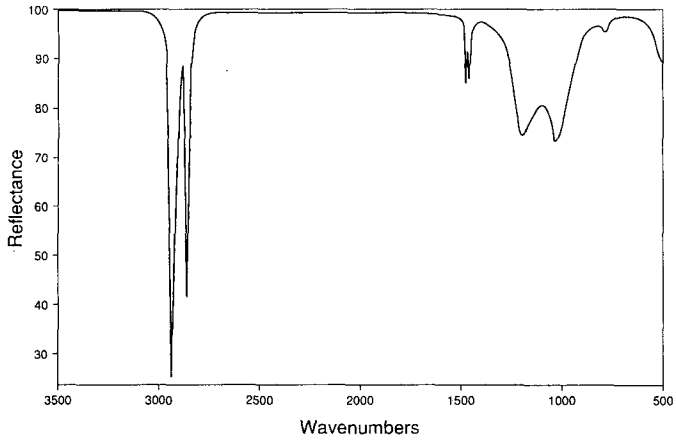

FIG. 13. Internal reflectance spectrum of a 500-Å-thick glass coating on polyethylene. Calculated at an incident angle of 45° and unpolarized radiation with a ZnSe IRE.

CONCLUSION

A generalized method has been compiled and implemented for fitting the optical constants to experimental spectra. This method utilizes a classical harmonic oscillator model for the vibrational modes and differs from the quantum mechanical description in terminology only; i.e., the resulting formulae are the same. It links the molecular polarizability, the optical constants, and the spectroscopic observables for which exact descriptions can be developed (i.e., transmission, external reflection, and internal reflection). As demonstrated by the polyethylene and glass examples, this method describes a wide variety of experimental conditions including spectroscopic technique, sample thickness, incident angle, and polarization.

With the use of this general formalism, various apparently different phenomena can be related and further investigated. The range and degree of validity of many phenomenological relationships (e.g., Beer's law) can be determined. Practical problems can undergo preliminary screening to determine the optimum conditions for experimental analysis.

1. P. J. Haysman and A. P. Lenham, J. Opt. Soc. of Am. **62,** 333 (1972).
2. R. T. Graf, J. L. Koenig, and H. Ishida, Anal. Chem. **58,** 64 (1988).
3. Y. Lu and A. Penzkofer, Appl. Opt. **25,** 221 (1986).
4. A. C. Gilby, J. Burr, Jr., W. Krueger, and B. Crawford, J. Phys. Chem. **70,** 1525 (1966).
5. W. N. Hansen, Spectrochim. Acta **21,** 815 (1965).
6. W. N. Hansen, Spectrochim. Acta **21,** 209 (1965).
7. W. N. Hansen, ISA Trans. **4,** 263 (1965).
8. J. Fahrenfort and W. M. Visser, Spectrochim. Acta **18,** 1103 (1962).
9. R. N. Jones, Chem. Rev. **71,** 218 (1971).
10. K. Ohta and H. Ishida, Appl. Spectrosc. **42,** 952 (1988).
11. D. L. Allara, A. Baca, and C. A. Pryde, Macromol. **11,** 1217 (1978).
12. H. R. Philipp and E. A. Taft, Phys. Rev. **113,** 1002 (1959).
13. K. Kozima, W. Suetaka, and P. N. Schatz, J. Opt. Soc. of Am. **56,** 181 (1966).
14. H. W. Verleur, J. Opt. Soc. of Am. **58,** 1356 (1968).
15. G. K. Ribbegard and R. N. Jones, Appl. Spectrosc. **34,** 638 (1980).
16. W. G. Spitzer and D. A. Kleinman, Phys. Rev. **121,** 1324 (1961).
17. J. M. Siqueiros, R. Machorro, and L. E. Regalado, Appl. Opt. **27,** 2549 (1988).
18. J. Pacansky, C. D. England, and R. Waltman, Appl. Spectrosc. **40,** 8 (1986).
19. J. R. Jasperse, A. Kahan, and J. N. Plendl, Phys. Rev. **146,** 526 (1966).
20. T. C. Paulick, Appl. Opt. **25,** 562 (1986).
21. F. Abeles, H. A. Washburn, and H. H. Soonpaa, J. Opt. Soc. of Am. **63,** 104 (1973).
22. E. B. Wilson, Jr., J. C. Decius, and P. C. Cross, *Molecular Vibrations* (McGraw-Hill, New York, 1955).
23. J. D. Jackson, *Classical Electrodynamics* (John Wiley and Sons, New York, 1975), 2nd ed.
24. M. Milosevic, N. J. Harrick, and S. L. Berets, Appl. Spectrosc. **45,** 126 (1991).
25. R. S. McDonald and P. A. Wilks, Jr., Appl. Spectrosc. **42,** 151 (1988).
26. *CRC Handbook of Chemistry and Physics,* R. C. Weast and M. J. Astle, Eds. (CRC Press, Boca Raton, Florida, 1981), 62nd ed.
27. N. J. Harrick, Appl. Spectrosc. **31,** 548 (1977).
28. *Optical Spectroscopy: Sampling Techniques Manual* (Harrick Scientific Corporation, Ossining, New York, 1978) and references therein.
29. C. Kittel, *Introduction to Solid State Physics* (John Wiley and Sons, New York, 1976), 5th ed.
30. Y.-S. Yen and J. S. Wong, Mikrochim. Acta **1,** 441 (1988).
31. J. Bandekar, private communications.